Graphene Terahertz Generators for Molecular Circuits and Sensors

Norma L. Rangel[†,‡] and Jorge M. Seminario*[,†,‡,§]

Department of Chemical Engineering, Materials Science and Engineering Graduate Program, and Department of Electrical and Computer Engineering, Texas A&M University, College Station, Texas

Received: September 14, 2008; Revised Manuscript Received: October 18, 2008

Using ab initio density functional theory methods, the optimized structure of the single-, double-, and triple-layered graphene nanoribbons with different stacking orders and edges is calculated along with their Raman spectrums. For each case studied, graphene is found to be a potential source of vibrational signals in the terahertz region of the spectrum when molecules or another layer are adsorbed in the surface; this effect is independent of the hydrogen presence at the edges, and the stacking order. The visible low-frequency modes increase with the addition of graphene layers, and the number of modes may be influenced by the type of edges. The monolayer shows better performance due to the lower number of vibrational modes. The nanoribbon with fewer modes at the terahertz range is used to show a potential application of graphene acting as a sensor of single molecules.

I. Introduction

Graphene is a "novel" material recently proposed as one of the main alternatives to overcome the performance limitations of materials such as silicon and carbon nanotubes. Graphene has been studied for more than 60 years,[1,2] but was only recently synthesized in 2004 by Novoselov et al.[3] They synthesized up to 10 μm lengths of single, double, and triple layer graphene structures by micromechanical cleavage of bulk graphite, attracting the interest of researchers to its properties and creating a potential usage for several applications. So far, several graphene properties are still unknown such as its toxicity, strength, hardness, toughness, porosity, phase diagram, and Curie point among others. Understanding graphene and its properties are important steps necessary to determine possible applications.

Vaporizing graphite by laser irradiation caused the quasi-0D carbon allotrope, fullerene, discovered in 1985 by Kroto et al,.[4] although some calculations were reported in 1970.[5] Using a similar method, the quasi-1D allotrope carbon nanotube (CNT) was officially discovered by Iijima in 1991;[6] however, some authors had reported this structure since 1952.[7] The starting material of the CNT structures is the two-dimensional single graphite sheet, graphene.

Graphene is a two-dimensional honeycomb network one atomic layer thick of sp^2 carbon atoms. Its unit cell contains only two atoms; however, when layers are coupled, the unit cell increases in two atoms per layer. The coupling of layers is due to the weak Van der Waals forces between them. The stacking order of these layers could potentially be the Bernal or hexagonal stacking (ABABAB...) or the rhombohedral stacking (ABCABC...), which can be considered as a planar defect of the Bernal stacking or simply no stacking order also known as turbostratic graphite.[8]

The number of layers, types of edges such as zigzag or armchair, and topological defects such as vacancies, impurities, ripples, nonhexagonal polygons, etc., affect the properties and behavior of the graphene crystals.[9,10] Structures with up to 10 graphene layers are known as few-layer graphenes (FLGs), while structures with more than 10 and less than 100 layers are considered as thin films of graphite.[11] The number of layers in a sample is very important and needs to be controlled because it may determine the properties and performance of the graphitic material. Initially, the number of layers of graphene was determined by using an optical microscope, placing the graphene over a SiO_2 substrate, and showing a tone color for different numbers of layers. The number of layers has been determined based on the height differences of images taken by a scanning tunneling microscopy (STM), using different substrates such as Si (100).[12]

The atomic lattice structure of a single graphene layer on a SiO_2 surface was characterized by Ishigami et al.[13] using a combination of STM for atomic scale resolution, atomic force microscope (AFM) to compare morphologies between the graphene and SiO_2, and scanning electron microscope (SEM) for rapid reproducible placement of the scanning probe. Some perturbations, meandering, and both triangular and hexagonal lattices were noticeable. These observations showed that graphene followed the SiO_2 morphology, and that any other substrate will also take priority over its intrinsic corrugation morphology, determined by Meyer et al.[14,15] using transmission electron microscopy (TEM) and freely suspending a graphene layer on top of micrometallic scaffolds.

Fabrication Methods. Starting with Brodie in 1859,[16] many different attempts have been made to produce FLGs. After the success of the "scotch tape" pealing technique used for its discovery,[3] the mechanical exfoliation technique[17] has been applied for this purpose. The mechanical exfoliation technique is a simple method in which the film thickness is determined based on the color of the SiO_2 substrate, but it is not appropriate for large-scale fabrication and the films produced are usually uneven. The SiO_2 thickness (300 nm), the initial graphite material (largest possible grains), and the graphite and SiO_2 surface quality (freshly cleaved and cleaned)[11] are critical aspects in the success of this method.

By applying an arc-discharge to silicon carbide (SiC) crystals, nanographite ribbons were fabricated in 2001,[18] using a hydrogen atmosphere to avoid the formation of pentagons and

* Corresponding author.
† Department of Chemical Engineering.
‡ Materials Science and Engineering Graduate Program.
§ Department of Electrical and Computer Engineering.

10.1021/jp808181n CCC: $40.75
Published on Web 12/04/2008

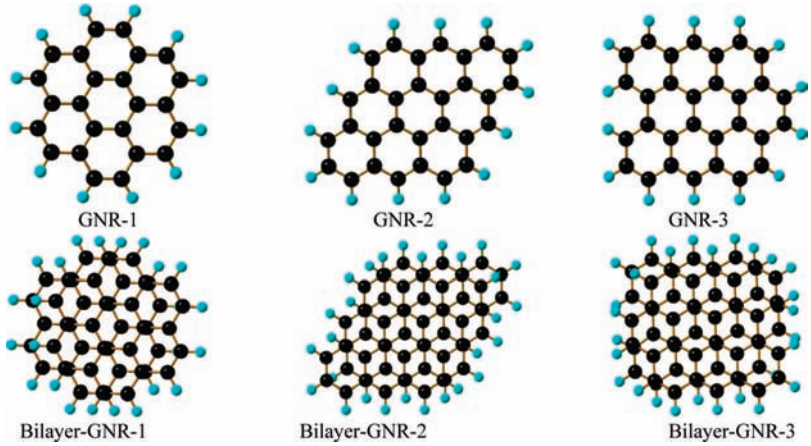

Figure 1. Graphene nanoribbons (GNRs) used considering different edge configurations: GNR-1, zigzag and armchair edges; GNR-2, monolayer graphene with both zigzag edges; and GNR-3, monolayer graphene with zigzag (horizontal) and armchair (vertical) edges. At the bottom the bilayer structures of GRN-1, GRN-2, and GRN-3 are shown. Black spheres are carbon atoms and blue spheres are hydrogen atoms.

TABLE 1: Monolayer and Bilayer Graphene Nanoribbons Results, Including Total Energy, Binding Energy (Between Layers), Dipole Moment, HOMO and LUMO Energies, HLGs, Number of Imaginary Frequencies, and Interlayer Distances

GNR mono/bi-layer	total energy (Ha)	binding energy (kcal/mol)	dipole moment (debye)	HOMO (eV)	LUMO (eV)	HLG (eV)	no. of Im freqs	interlayer distance (Å)
GNR-1	−921.841934		0.00	−6.67	−0.63	6.04	0	
Bilayer-GNR-1	−1843.702717	−11.83	0.00	−6.31	−0.63	5.69	0	3.45
GNR-2	−1151.680690		0.00	−5.61	−1.77	3.84	0	
Bilayer-GNR-2	−2303.386572	−15.81	0.00	−5.36	−1.82	3.54	0	3.38
GNR-3	−1151.693127		0.10	−5.77	−1.61	4.16	0	
Bilayer-GNR-3	−2303.410458	−15.19	0.00	−5.44	−1.55	3.89	1	3.45

therefore the nonplanar structures. This procedure eventually inspired the currently known epitaxial graphite fabrication technique,[19] where the SiC crystal is heated to about 1300°C in an ultrahigh vacuum, leading to the growth of FLGs with at least 5 layers and up to 100 layers. Since this is a thermal product, it is hard to functionalize these films for industrial applications. The high temperature is an inconvenience that is also present in the attempt to obtain FLG by heating diamond nanoparticles in an inert argon atmosphere.[20] In this treatment, the required temperature is about 1650 °C.[21]

Chemical vapor deposition (CVD) is another strategy proposed to fabricate FLGs. One case of CVD is using camphor, which is heated between 700 and 850°C, pyrolyzed, and collected in nickel substrates.[22] The CVD method is more practical for industrial applications but still not effective for the functionalization of films, and it is currently viable only on metal surfaces.[21,23]

The exfoliation (i.e., peeling away the layers) of graphite oxide, however, seems to be a very promising technique for large-scale fabrication of functionalized single graphite layers.[24] This method consists of treating graphite with concentrated acids to obtain a sufficient oxidation of the graphite, and then thermally exfoliating at about 1050 °C.[21] Some of the difficulties of this method are to obtain the optimal oxidation and an adequate pressure during the heat treatment to reduce the possibility of having partially oxidized layers.

So far the best method to obtain the single layer graphene is the mechanical exfoliation technique or mechanical cleavage, particularly for research. It is cheap, simple, and does not require any extreme pressure or temperature conditions. However, this technique is not good for large-scale fabrication and sometimes the sample obtained may be uneven. For large-scale production the exfoliation of graphite oxide technique can be used. It can produce films in large scale but some stabilization treatment needs to be done, because the graphene obtained tends to agglomerate and becomes hard to functionalize.

Properties. The effective spring constants of a FLG (less than 5 layers)[25] and graphene membranes (8 to 100 layers)[26] have been experimentally measured by using an AFM under ambient conditions. The AFM tip is calibrated and pressed over the suspended stacks of graphene sheets. Spring constants vary from 1 to 5 N/m for samples with thickness between 2 and 8 nm. From these data the Young's modulus is estimated to be 0.5 TPa for both FLG and graphene membranes, which is half of the reported value for graphite along the basal plane.[27] After determining the FLG's Young modulus, a resonator was fabricated with a single layer graphene, producing modulus values between 53 and 170 GPa,[28] similar to those of single-wall carbon nanotubes[29] and diamond. In 2008, Lee et al.[30] by nanoindentation measured the elastic properties and intrinsic strength obtaining values corresponding to a Young's modulus of 1TPa, positioning the monolayer graphene as one of the strongest materials ever measured. Despite the fact that a lot of work has been done to determine the mechanical properties of the carbon nanotubes,[29] the study of the mechanical properties of the unrolled structure, graphene, is still in its infant stage, and so far most of the experiments on graphene have focused only on their electronic properties.[31]

By using the tight binding model, the band structure of graphene was calculated first by Wallace in 1946,[1] and again by others in recent reports.[31] It has been shown that graphene is a zero gap semimetal and graphite is a semimetal with a band overlap of 41 meV.[32] After the discovery of graphene, several experiments have been performed to determine its electrical properties. Novoselov et al.[3] applied an external gate bias on samples with single and double layers by placing gold electrodes on top of the graphene. The single graphene and its bilayer showed a tunable semiconductor behavior.[31,33−35] The band gap

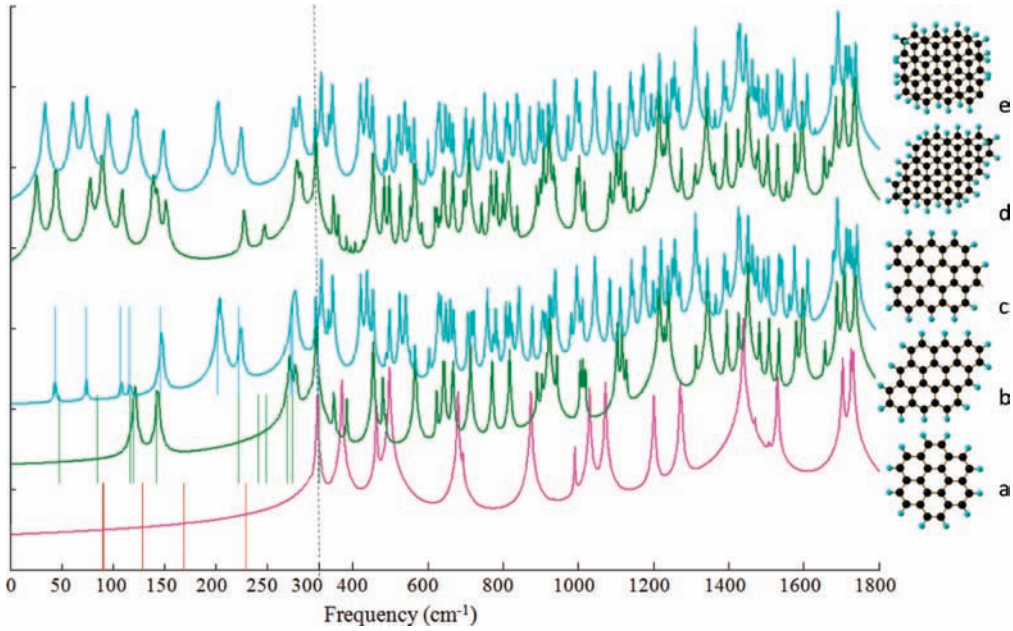

Figure 2. Frequency spectrum for the nanoribbons described in Figure 1. From bottom to top the spectrum of GNR-1 (pink), GNR-2 (green), GNR-3 (blue), bilayer GNR-2 (green), and bilayer-GNR-3 (blue).

can be modulated upward until a minimum conductivity value is reached for all FLG; bandgaps cannot be modulated enough to force the FLG to act as an insulator. It is noted that the band gap depends on the impurity concentrations and the presence of a substrate.[36] The behavior of graphene can be regarded as ballistic with mobilities in excess of 200 000 $cm^2\ V^{-1}\ s^{-1}$ for electron concentrations of approximately $2 \times 10^{11}\ cm^{-2}$, [37] and a scattering distance around 0.3 μm.[11] These high mobility values are found to be independent of chemical and electrical doping.

In contrast to quantum chemistry theory, where all interactions are treated by real (actual) Hamiltonians derived from first principles (ab initio) following a bottom-up approach, most condensed matter treatments are top-down approaches, which necessarily requires experimental information and therefore the creation of phenomenological or empirical Hamiltonians. Thus for the particular case of graphene, some authors have found that electric transport is better described by pseudoparticles responding to a phenomenological relativistic equation.[38,39] This is because graphene low-energy excitations are like massless Dirac−Fermions[11,40,41] that can explain the particular fractional quantum Hall effect, observed at room temperatures.[42]

Experiments have revealed the effect of a magnetic field in single graphene and FLGs, producing a peculiar room temperature quantum Hall effect. Theoretically, graphite's diamagnetism[43,44] and shortly later graphene's diamagnetism[45] were studied, and found to increase at low temperatures.[44] Calculations of graphene nanoislands show that the shape of the edges (zigzag or arm-chair)[46] influences the magnetic properties, resulting in the zigzag system behaving as diamagnetic at high temperatures but as paramagnetic at low temperatures.[10]

Such properties can be presented in carbon nanotubes by using materials like Fe filling the tube. The presence of undercoordinated carbon atoms similar to the carbons in the zigzag edges in graphene present this ferromagnetic behavior in carbon-based structures[47,48] but this is not enough to define the magnetic properties of the material, for the carbon nanotubes case, the magnetic properties are chirality, diameter, and length dependent,[49] and the presence of vacancies[50] or adatoms[51] also affects the magnetic properties of carbon nanotubes.

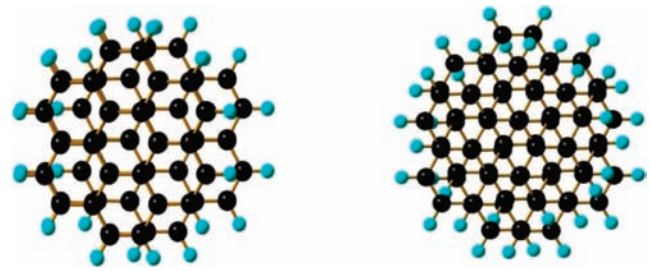

Figure 3. Clusters of three layers of GNR-1 passivated by using hydrogen atoms (blue): (left) top view of a trilayer graphene, using Bernal stacking ABAB... and (right) top view of trilayer graphene with rhombohedral stacking order ABCABC....

As a result of these modifiable magnetic properties, an opportunity to obtain engineered magnetic materials has been proposed,[52] which consists of graphene superlattices patterned with nanoholes of different shapes and sizes and producing a material with combined semiconductor-magnetic behavior.

An experiment was recently (2008) performed by Nair et al.[53] where wavelengths between 250 and 1200 nm were focused on a sample consisting of a suspended single and double layer graphene, showing that the difference in opacity increases by 2.3% for each layer of graphene added. Variations in the wavelength did not show any effect in the opacity measurements, which implies that even white light can be used to perform the experiment.

Applications. The exceptional properties found for graphene suggest that the one atom thick crystal is an excellent candidate for a wide range of applications.[11] It is sufficient to take a look at the large amount of already proposed applications for carbon nanotubes for example in photonics,[54] as composite materials[55] among others, and study the possibility of replacing them with the two-dimensional structure, graphene, which has already shown similar and better properties resulting in an improved performance in most of those applications.[37,56]

Graphene offers several advantages over current electronic devices. Starting with the electrical properties, graphene is projected to be the material of choice to replace silicon, which is now reaching its physical limits, opening a potential carbon-

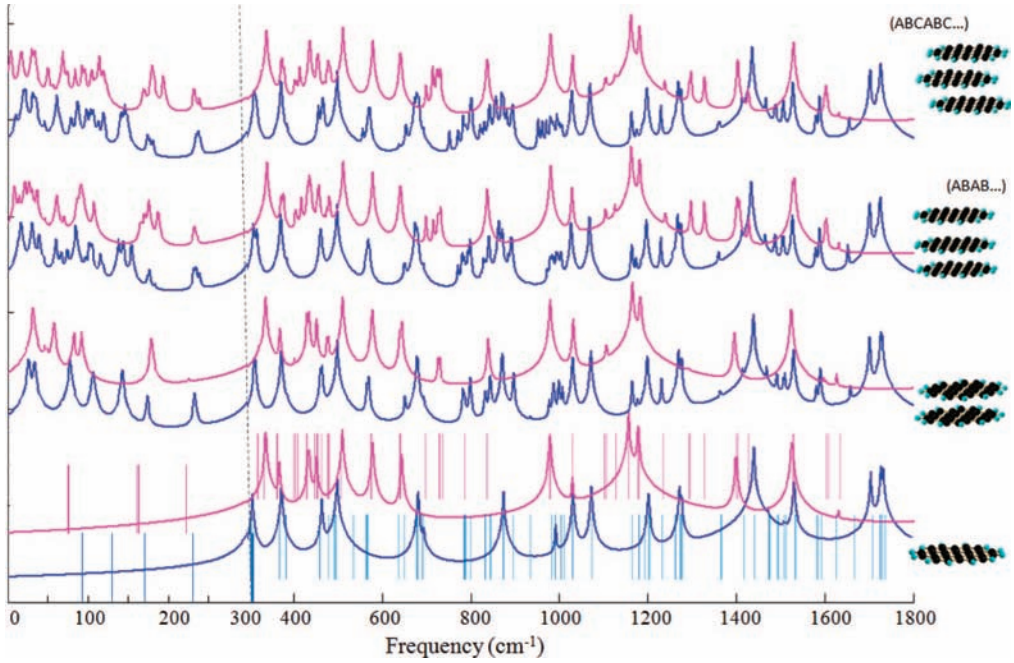

Figure 4. Graphene nanoribbons as a source of terahertz signals. Both hydrogen passivated and nonpassivated structures show that the frequency spectrum for a single graphene layer starts at frequencies greater than 300 cm^{-1}, while the second and third layered cluster structures show Raman intensities in the terahertz region (less than 100 cm^{-1}). Vertical lines in the two lower spectra show all the nonactive and active Raman vibrational modes.

based electronics era. With mobilities that are five times larger in suspended graphene[37] than in silicon, graphene offers faster devices with lower energy dissipation due to its ballistic behavior,[57] and with less noise than most semiconductors by using the bilayer graphene.[58] Field effect transistors,[59] single electron transistors,[60] pn junctions,[61] pnp junctions,[62] and binary memory devices[63] have been fabricated. A graphene spin valve[64] showing giant magnetoresistance has also been fabricated, offering the possibility of using graphene for spintronics applications.

Applications in nanoelectromechanical systems (NEMS) such as resonators and high-pressure sensors have been proposed, based on its mechanical properties.[28] Graphene-based composite materials have been suggested,[65] and have recently shown exceptional results,[56] where the glass transition temperature for poly(acrylonitrile) and poly(methyl methacrylate) has been improved by approximately 40 and 30 °C, using only 1 and 0.05 wt % of functionalized graphene sheets, respectively.

The possibility of using graphene as a molecular sensor has been experimentally proven by Scheding et al.[66] resulting in a change in conductivity when gas molecules such as NO_2, NH_3, H_2O, and CO with different concentrations are adsorbed on a graphene surface. This was later theoretically demonstrated by Hwang et al. for NO_2 and NH_3[67] finding a high sensitivity, low noise, and room temperature operated sensor.

Fabrication of large graphene membranes, currently up to 100 μm,[68] has opened the door to the possibility of measuring more properties experimentally, and their use on other applications. Large size membranes facilitate the study of the mechanical properties in graphene. Graphene impermeability to the second smallest atomic gas helium suggested that graphene membranes can be used as interfaces separating even two different phases of matter.[69] On the other hand, their potential as a molecular filter can be reached by patterning with an electron beam different diameter holes in the graphene membrane acting like a sieve or mesh that separate wanted from unwanted molecules, but this is an approach that has not been fully explored.

Applications of graphene for hydrogen storage,[70] spin filters,[71] electrodes in solar cells,[72] batteries, emitters, and even in quantum computing have been suggested and/or reported in the last year.[11] Still, several potential applications of graphene synthesized just four year ago are unknown, and questions regarding its behavior, performance, and properties in the already proposed applications are still unanswered.

One possible application of graphene is to use it as a molecular sensor by using molecular vibrations (vibronics).[73] Vibronics can be used to sense or transport signals and theoretical simulations have shown the possible use for sensors to identify single molecules with modes in the terahertz (THz) region. The vibrational spectrum of monolayer and multilayer graphene, characterization, along with its applications as part of a molecular circuit are the main topics focused on in this paper.

II. Methodology

By using ab initio density functional theory with the hybrid functional M05-2X, which has an improved performance for

TABLE 2: Total Energy, Binding Energy (Between Layers), Dipole Moment, HOMO and LUMO Energies, HLG, Number of Imaginary Frequencies, and Interlayer Distances for the GNR-1 Clusters Used for Vibronics

trilayer GNR-1 stacking	total energy (Ha)	binding energy (kcal/mol)	dipole moment (debye)	HOMO (eV)	LUMO (eV)	HLG (eV)	no. of Im freq	interlayer distance (Å)
ABA	−2765.562167	−22.82	0.04	−6.10	−0.54	5.55	2	3.43
ABC	−2765.562937	−23.30	0.04	−6.12	−0.57	5.55	0	3.44

TABLE 3: Total Energy, Binding Energy (Absorption of N_2), Dipole Moment, HOMO and LUMO Energies, HLG, and Number (Value) of Imaginary Frequencies for the Graphene Clusters with N_2

GNR-1	total energy (Ha)	binding energy (kcal/mol)	dipole moment (debye)	HOMO (eV)	LUMO (eV)	HLG (eV)	no. of Im freqs
monolayer-N_2	−1031.358712	−1.51	0.08	−6.67	−0.65	6.01	1 (−46.68i)
bilayer-N_2	−1953.220201	−1.95	0.09	−6.31	−0.63	5.69	1 (−7.08i)
trilayer-N_2 (ABAB...)	−2875.079784	−2.04	0.11	−6.12	−0.54	5.58	1 (−8.11i)
trilayer-N_2 (ABCABC...)	−2875.080712	−2.14	0.10	−6.12	−0.57	5.55	0

TABLE 4: Total Energy, Binding Energy (Absorption of O_2), Dipole Moment, HOMO and LUMO Energies, HLG, Number (Value) of Imaginary Frequencies for the Graphene Clusters with O_2

GNR-1	total energy (Ha)	binding energy (kcal/mol)	dipole moment (debye)	HOMO (eV)		LUMO (eV)		HLG (eV)	no. of Im freqs
				α	β	α	β		
monolayer-O_2	−1072.139125	−1.72	0.02	−6.67	−6.67	−0.63	−0.73	5.93	0
bilayer-O_2	−1994.000466	−2.07	0.02	−6.29	−6.29	−0.60	−0.63	5.66	0
trilayer-O_2 (ABAB...)	−2915.859914	−2.06	0.04	−6.10	−6.10	−0.54	−0.54	5.55	0
trilayer -O_2 (ABCABC...)	−2915.861017	−2.27	0.04	−6.12	−6.12	−0.57	−0.57	5.55	0

nonbonded interactions and $\pi-\pi$ stacking,[74] the optimized structure of the single-, double-, and triple-layered graphene nanoribbons (GNRs) shown in Figure 1 are calculated. All calculations are performed with the 6-31G(d) basis, using the program Gaussian 03 (revision E01).[75] Once the optimized geometries are found, the Raman spectrum is calculated.

The coupling between graphene layers is evaluated through the binding energies, i.e., difference between the total energy of the optimized cluster with the energies sum of the optimized individual layers. The total and binding energies, highest occupied molecular orbital (HOMO) and the lowest unoccupied molecular orbital (LUMO) energies, HOMO-LUMO gap (HLG) energies, along with their imaginary frequencies and the distance between layers obtained for the optimized structures shown in Figure 1 are presented in Table 1.

The only imaginary frequency (11.1*i*) is obtained for the bilayer GNR-3. The interlayer distance is shorter for the GNR with zigzag edges and the binding energy is slightly affected by them. The GNRs shown in Figure 1 are also calculated without hydrogen atoms at the edges (nonpassivated structures), and the binding energy is 0.5 kcal/mol stronger, since the hydrogen−hydrogen repulsion is eliminated from the system. The HLGs are shorter in the bilayer compared with the single layer for each GNR case (the effect of the edges in the HLG is noticed by comparing GNR-2 and GNR-3), larger gap is presented with armchair edges than with zigzag edges, and finally the gap is also affected by the number of carbon atoms (as is noticed by comparing GNR-1 with GNR-2 and GNR-3), and with a larger number of carbons the HLG trends to decrease.

The symmetry of the GNR-1 and GNR-2 is C_{2v}, and for GNR-3 it is C_1. As is shown in Figure 2, modes without Raman amplitude are presented at low frequencies for the ribbons with C_{2v}. They are all visible for the graphene with C_1. None of the monolayer GNRs show either visible or hidden modes of frequencies in the range lower than 50 cm^{-1}. The GNR-1 does not present any visible mode for frequencies lower than 300 cm^{-1}, and for this reason this is the ribbon used for the sensing calculations.

III. Vibronics

Currently, graphene nanoribbons (GNRs) with less than 10 nm width can be fabricated and used as semiconductors.[76] Their Raman spectra have been determined experimentally for different numbers of layers.[77] With this information, an opportunity for new graphene applications is presented here: a sensor in the terahertz region.

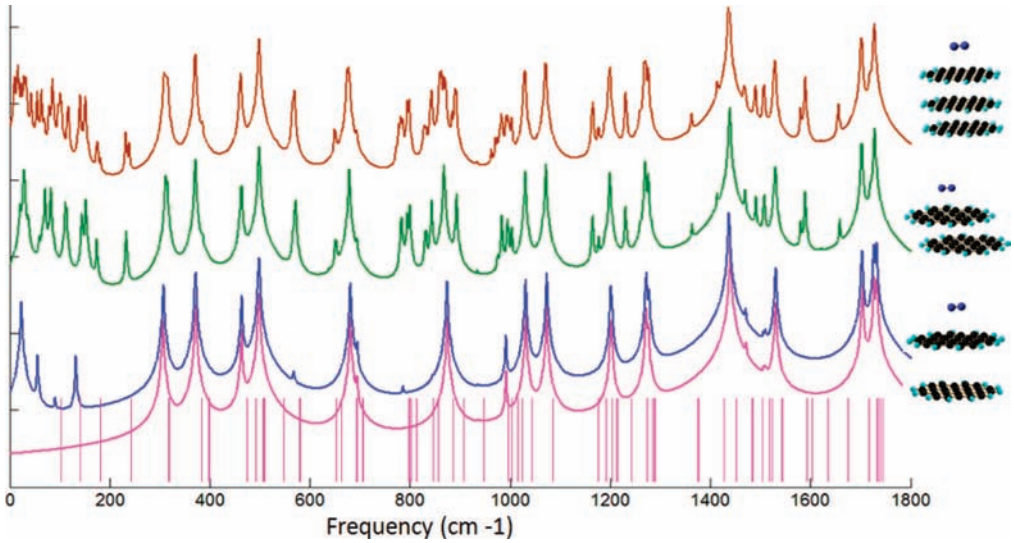

Figure 5. Frequency spectrum for graphene nanoribbons acting as sensors of single molecules N_2 with terahertz fingerprints. From bottom to top: GNR-1 frequency modes (pink vertical lines) and its Raman spectrum (pink), spectrum of GNR-1 with N_2 adsorbed (blue), bilayer GNR-1 adsorbing N_2 (green), and trilayer GNR-1 adsorbing N_2 (brown).

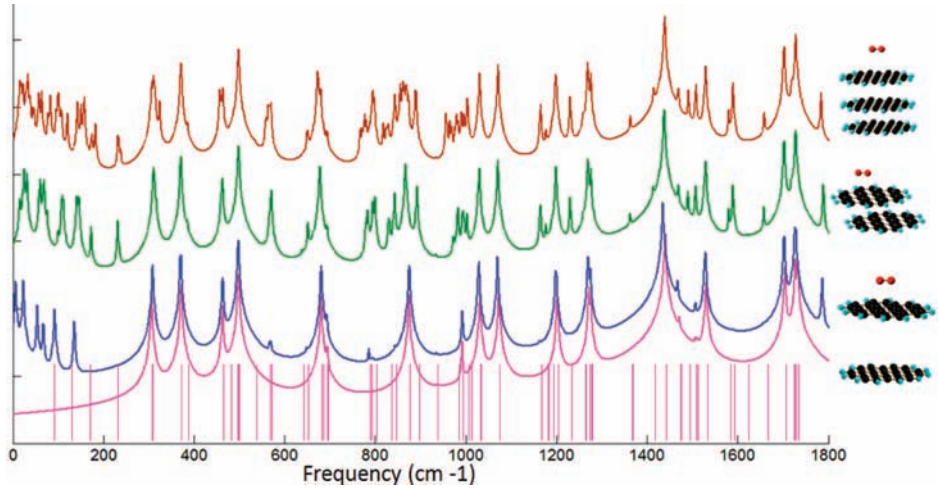

Figure 6. Frequency spectrum for graphene nanoribbons acting as sensors of single molecules O_2 with terahertz fingerprints. From bottom to top: GNR-1 frequency modes (pink vertical lines) and its Raman spectrum (pink), spectrum of GNR-1 with O_2 adsorbed (blue), bilayer GNR-1 adsorbing O_2 (green), and trilayer GNR-1 adsorbing O_2 (brown).

The GNR-1 and its bilayer shown in Figure 1 with the trilayer clusters GNR-1 using Bernal and rhombohedral stackings shown in Figure 3 are used to detect the presence of an adsorbed molecule in their surfaces.

The energies for the trilayer clusters of GNR-1 are shown in Table 1, in the same way as for the monolayer and bilayer shown in Table 2.

Imaginary frequencies are obtained for the trilayer with Bernal stacking (ABA) with values 10.8*i* and 5.2*i*. The binding energy is slightly affected by the stacking order being ~0.5 kcal/mol stronger in the Bernal stacking.

Raman intensities for low frequencies are shown in Figure 4, for both passivated (blue lines) and nonpassivated (pink lines) structures of the monolayer, bilayer, and trilayer GNR. Fewer modes are present when there are no hydrogen passivations in the clusters; as expected, if the number of layers increases the number of modes also increases and so does the number of modes generated at the low frequencies.

IV. Sensing Molecules in the Terahertz Region

The appearance of THz modes in the graphene spectrum occurs when molecules are adsorbed in the surface, even if the molecules do not have a signature in such a region. These characteristic peaks can be used as THz fingerprints of single molecules. Even though the effect of temperature and the substrate on the graphene Raman spectroscopy is still unclear,[78] its room temperature vibrational modes could be used as sensors of single molecules and the FLG as a generator of THz signals. Certainly, vibronics is only one of several possible graphene applications; however, as ideas emerge daily they are being developed and integrated into our current research.

The optimized GNR-1 and its bilayer and trilayer (Bernal and rhombohedral) clusters are used as sensors of molecules. The molecules adsorbed in the surfaces are O_2 and N_2 for the sake of proof-of-concept; their small size facilitates the calculations, but this approach can be extended to any molecule. Each cluster is optimized with the adsorbed molecule. Total energies of the structures, HOMO, LUMO, and HLG energies along with the binding energies of the sensed molecules, i.e., the N_2 or O_2, are shown in Tables 3 and 4, respectively.

The Raman spectra of the clusters with molecules adsorbed in the surface is calculated and is compared with the spectrum for the GNR-1 before the presence of molecules N_2 and O_2 and are shown respectively in Figures 5 and 6. Hidden and visible modes in the range lower than 300 cm^{-1} are compared for each cluster before and after the adsorption of molecules, also the modes generated by adding more layers are considered.

At 29.2 cm^{-1} there is a mode corresponding to the nitrogen molecule, which appears for the single, double, and triple layer. Other characteristic modes can be identified as fingerprints of the molecule sensed depending on the number of graphene layers used.

Between 23 and 25 cm^{-1} a mode appears in each GNR cluster due to the presence of the oxygen molecule.

V. Conclusions

The interaction between graphene layers yields vibrational modes in the terahertz region of the spectrum, independent of the type of edges, the presence of hydrogen pasivating the layers, or the number of layers. The presence of molecules on a graphene membrane can be detected from its vibrational modes in the terahertz spectrum. The interlayer distance of ribbons with zigzag edges is shorter. However, binding energies are slightly affected by the edge passivation with hydrogen: 2.5 kcal/mol stronger binding when there is not hydrogen. Also the binding energy is slightly affected by the stacking order: ~0.5 kcal/mol stronger in the Bernal stacking.

Acknowledgment. We acknowledge financial support from the U.S. Army Research Office and the U.S. Defense Threat Reduction Agency (DTRA).

References and Notes

(1) Wallace, P. R. *Phys. Rev.* **1947**, *71*, 622.
(2) Slonczewski, J. C.; Weiss, P. R. *Phys. Rev.* **1958**, *109*, 272.
(3) Novoselov, K. S.; Geim, A. K.; Morozov, S. V.; Jiang, D.; Zhang, Y.; Dubonos, S. V.; Grigorieva, I. V.; Firsov, A. A. *Science* **2004**, *306*, 666.
(4) Kroto, H. W.; Heath, J. R.; O'Brien, S. C.; Curl, R. F.; Smalley, R. E. *Nature* **1985**, *318*, 162.
(5) Kroto, H. *J. Mol. Graphics Modell.* **2001**, *19*, 187.
(6) Iijima, S. *Nature* **1991**, *354*, 56.
(7) Monthioux, M.; Kuznetsov, V. L. *Carbon* **2006**, *44*, 1621.
(8) Delhaes, P. *Graphite and precursors*; Gordon & Breach; Amsterdam, The Netherlands, 2000.
(9) Hashimoto, A.; Suenaga, K.; Gloter, A.; Urita, K.; Iijima, S. *Nature* **2004**, *430*, 870.
(10) Wakabayashi, K.; Fujita, M.; Ajiki, H.; Sigrist, M. *Phys. Rev. B* **1999**, *59*, 8271.

(11) Geim, A. K.; Novoselov, K. S. *Nat. Mater* **2007**, *6*, 183.
(12) Ritter, K. A.; Lyding, J. W. *Nanotechnology* **2008**, *19*, 015704.
(13) Ishigami, M.; Chen, J. H.; Cullen, W. G.; Fuhrer, M. S.; Williams, E. D. *Nano Lett.* **2007**, *7*, 1643.
(14) Meyer, J. C.; Geim, A. K.; Katsnelson, M. I.; Novoselov, K. S.; Booth, T. J.; Roth, S. *Nature* **2007**, *446*, 60.
(15) Meyer, J. C.; Geim, A. K.; Katsnelson, M. I.; Novoselov, K. S.; Obergfell, D.; Roth, S.; Girit, C.; Zettl, A. *Solid State Commun.* **2007**, *143*, 101.
(16) Brodie, B. C. *Philos. Trans. R. Soc. London* **1859**, *149*, 249.
(17) Chung, D. D. L. *J. Mater. Sci.* **1987**, *22*, 4190.
(18) Li, Y.; Xie, S.; Zhou, W.; Tang, D.; Zou, X.; Liu, Z.; Wang, G. *Carbon* **2001**, *39*, 626.
(19) de Heer, W. A.; Berger, C.; Wu, X.; First, P. N.; Conrad, E. H.; Li, X.; Li, T.; Sprinkle, M.; Hass, J.; Sadowski, M. L.; Potemski, M.; Martinez, G. *Solid State Commun.* **2007**, *143*, 92.
(20) Andersson, O. E.; Prasad, B. L. V.; Sato, H.; Enoki, T.; Hishiyama, Y.; Kaburagi, Y.; Yoshikawa, M.; Bandow, S. *Phys. Rev. B* **1998**, *58*, 16387.
(21) Subrahmanyam, K. S.; Vivekchand, S. R. C.; Govindaraj, A.; Rao, C. N. R. *J. Mater. Chem.* **2008**, *18*, 1517.
(22) Somani, P. R.; Somani, S. P.; Umeno, M. *Chem. Phys. Lett.* **2006**, *430*, 56.
(23) Coraux, J.; Ndiaye, A. T.; Busse, C.; Michely, T. *Nano Lett.* **2008**, *8*, 565.
(24) Stankovich, S.; Dikin, D. A.; Piner, R. D.; Kohlhaas, K. A.; Kleinhammes, A.; Jia, Y.; Wu, Y.; Nguyen, S. T.; Ruoff, R. S. *Carbon* **2007**, *45*, 1558.
(25) Frank, I. W.; Tanenbaum, D. M.; Zande, A. M. v. d.; McEuen, P. L. *J. Vacuum Sci. Technol. B: Microelectron. Nanometer Struct.* **2007**, *25*, 2558.
(26) Poot, M.; Zant, H. S. J. v. d. *Appl. Phys. Lett.* **2008**, *92*, 063111.
(27) Kelly, B. T. *Physics of graphite*; Applied Science Publishers: London, 1981.
(28) Bunch, J. S.; van der Zande, A. M.; Verbridge, S. S.; Frank, I. W.; Tanenbaum, D. M.; Parpia, J. M.; Craighead, H. G.; McEuen, P. L. *Science* **2007**, *315*, 490.
(29) Dong, Q.; Gregory, J. W.; Wing Kam, L.; Min-Feng, Y.; Rodney, S. R. *Appl. Mech. Rev.* **2002**, *55*, 495.
(30) Lee, C.; Wei, X.; Kysar, J. W.; Hone, J. *Science* **2008**, *321*, 385.
(31) Neto, A. H. C.; Guinea, F.; Peres, N. M. R.; Novoselov, K. S.; Geim, A. K. *Condens. Matter* In press;arXiv:0709.1163v1.
(32) Partoens, B.; Peeters, F. M. *Phys. Rev. B* **2006**, *74*, 075404.
(33) Edward, M. *Phys. Rev. B (Condens. Matter Mater. Phys.)* **2006**, *74*, 161403.
(34) Edward, M.; Vladimir, I. F. K. *Phys. Rev. Lett.* **2006**, *96*, 086805.
(35) Castro, E. V.; Novoselov, K. S.; Morozov, S. V.; Peres, N. M. R.; Lopes dos Santos, J. M. B.; Nilsson, J.; Guinea, F.; Geim, A. K.; Castro Neto, A. H. *Phys. Rev. Lett.* **2007**, *99*, 216802.
(36) Adam, S.; Sarma, S. D. *Solid State Commun.* **2008**, *146*, 356.
(37) Bolotin, K. I.; Sikes, K. J.; Jiang, Z.; Klima, M.; Fudenberg, G.; Hone, J.; Kim, P.; Stormer, H. L. *Solid State Commun.* **2008**, *146*, 351.
(38) Peres, N. M. R.; Guinea, F.; Neto, A. H. C. *Phys. Rev. B (Condens. Matter Mater. Phys.)* **2006**, *73*, 125411.
(39) Dirac, P.A. M. *Proc. R. Soc. London. Ser. A* **1928**, *117*, 610.
(40) Novoselov, K. S.; Geim, A. K.; Morozov, S. V.; Jiang, D.; Katsnelson, M. I.; Grigorieva, I. V.; Dubonos, S. V.; Firsov, A. A. *Nature* **2005**, *438*, 197.
(41) Zhou, S. Y.; Gweon, G. H.; Graf, J.; Fedorov, A. V.; Spataru, C. D.; Diehl, R. D.; Kopelevich, Y.; Lee, D. H.; Louie, S. G.; Lanzara, A. *Nat. Phys.* **2006**, *2*, 595.
(42) Zhang, Y.; Tan, Y.-W.; Stormer, H. L.; Kim, P. *Nature* **2005**, *438*, 201.
(43) Mrozowski, S. *Phys. Rev.* **1952**, *86*, 1056.
(44) Sharma, M. P.; Johnson, L. G.; McClure, J. W. *Phys. Rev. B* **1974**, *9*, 2467.
(45) McClure, J. W. *Phys. Rev.* **1956**, *104*, 666.
(46) Fernandez-Rossier, J.; Palacios, J. J. *Phys. Rev. Lett.* **2007**, *99*, 177204.
(47) Makarova, T. L.; Sundqvist, B.; Hohne, R.; Esquinazi, P.; Kopelevich, Y.; Scharff, P.; Davydov, V. A.; Kashevarova, L. S.; Rakhmanina, A. V. *Nature* **2001**, *413*, 716.
(48) Kim, Y.-H.; Choi, J.; Chang, K. J.; Tománek, D. *Phys. Rev. B* **2003**, *68*, 125420.
(49) Krompiewski, S.; Cuniberti, G. *J. Magn. Magn. Mater.* **2007**, *310*, 2439.
(50) Ma, Y.; Lehtinen, P. O.; Nieminen, R. M. *New J. Phys.* **2004**, *6*, 68.
(51) Lehtinen, P. O.; Foster, A. S.; Ayuela, A.; Vehviläinen, T. T.; Nieminen, R. M. *Phys. Rev. B* **2004**, *69*, 155422.
(52) Yu, D.; Lupton, E. M.; Liu, M.; Liu, W.; Liu, F. Magnetic Graphene Nanohole Superlattices, 2008, submitted for publication.
(53) Nair, R. R.; Blake, P.; Grigorenko, A. N.; Novoselov, K. S.; Booth, T. J.; Stauber, T.; Peres, N. M. R.; Geim, A. K. *Science* **2008**, *320*, 1308.
(54) Avouris, P.; Freitag, M.; Perebeinos, V. *Nat. Photon* **2008**, *2*, 341.
(55) Thostenson, E. T.; Ren, Z.; Chou, T.-W. *Compos. Sci. Technol.* **2001**, *61*, 1899.
(56) Ramanathan, T.; Abdala, A. A.; Stankovich, S.; DikinD, A.; Herrera-Alonso, M.; Piner, R. D.; Adamson, D. H.; Schniepp, H. C.; Chen, X.; Rouff, R. S.; Nguyen, S. T.; Aksay, I. A.; Prud'homme, R. K.; Brinson, L. C. *Nature* **2008**, *3*, 327.
(57) Gunlycke, D.; Lawler, H. M.; White, C. T. *Phys. Rev. B (Condens. Matter Mater. Phys.)* **2007**, *75*, 085418.
(58) Lin, Y.-M.; Avouris, P. *Nano Lett.* **2008**, in press.
(59) Echtermeyer, T. J.; Lemme, M. C.; Bolten, J.; Baus, M.; Ramsteiner, M.; Kurz, H. *Eur. Phys. J.—Special Topics* **2007**, *148*, 19.
(60) Ponomarenko, L. A.; Schedin, F.; Katsnelson, M. I.; Yang, R.; Hill, E. W.; Novoselov, K. S.; Geim, A. K. *Science* **2008**, *320*, 356.
(61) Abanin, D. A.; Levitov, L. S. *Science* **2007**, *317*, 641.
(62) Barbaros, O.; Pablo, J.-H.; Dmitri, E.; Dmitry, A. A.; Leonid, S. L.; Philip, K. *Phys. Rev. Lett.* **2007**, *99*, 166804.
(63) Gunlycke, D.; Areshkin, D. A.; Li, J.; Mintmire, J. W.; White, C. T. *Nano Lett.* **2007**, *7*, 3608.
(64) Hill, E. W.; Geim, A. K.; Novoselov, K.; Schedin, F.; Blake, P. *Magn., IEEE Trans.* **2006**, *42*, 2694.
(65) Stankovich, S.; Dikin, D. A.; Dommett, G. H. B.; Kohlhaas, K. M.; Zimney, E. J.; Stach, E. A.; Piner, R. D.; Nguyen, S. T.; Ruoff, R. S. *Nature* **2006**, *442*, 282.
(66) Schedin, F.; Geim, A. K.; Morozov, S. V.; Hill, E. W.; Blake, P.; Katsnelson, M. I.; Novoselov, K. S. *Nat. Mater.* **2007**, *6*, 652.
(67) Hwang, E. H.; Adam, S.; Sarma, S. D. *Phys. Rev. B (Condens. Matter Mater. Phys.)* **2007**, *76*, 195421.
(68) Booth, T. J.; Blake, P.; Nair, R. R.; Jiang, D.; Hill, U.; Bangert, E. W.; Bleloch, A.; Gass, M.; Novoselov, K. S.; Katsnelson, M. I.; Geim, A. K. In press; arXiv:0803.37182008.
(69) Bunch, J. S.; Verbridge, S. S.; Alden, J. S.; van der Zande, A. M.; Parpia, J. M.; Craighead, H. G.; McEuen, P. L. *cond-mat.mtrl-sci* **2008**, in press; arXiv:0805.3309v1.
(70) Jorge, O. S.; Ajay, S. C.; Greg, D. B. *Phys. Rev. B (Condens. Matter Mater. Phys.)* **2007**, *75*, 153401.
(71) Karpan, V. M.; Giovannetti, G.; Khomyakov, P. A.; Talanana, M.; Starikov, A. A.; Zwierzycki, M.; Brink, J. v. d.; Brocks, G.; Kelly, P. J. *Phys. Rev. Lett.* **2007**, *99*, 176602.
(72) Wang, X.; Zhi, L. J.; Tsao, N.; Tomovic, Z.; Li, J. L., Mallen, K. Transparent carbon films as electrodes in organic solar cells, in press, 2008.
(73) Seminario, J. M.; Yan, L.; Ma, Y. *Proc. IEEE* **2005**, *93*, 1753.
(74) Zhao, Y.; Schultz, N. E.; Truhlar, D. G. *J. Chem. Theory Comput.* **2006**, *2*, 364.
(75) Frisch, M. J.; Trucks, G. W.; Schlegel, H. B.; Scuseria, G. E.; Robb, M. A.; Cheeseman, J. R.; Montgomery, J. A., Jr.; Vreven, T.; Kudin, K. N.; Burant, J. C.; Millam, J. M.; Iyengar, S. S.; Tomasi, J.; Barone, V.; Mennucci, B.; Cossi, M.; Scalmani, G.; Rega, N.; Petersson, G. A.; Nakatsuji, H.; Hada, M.; Ehara, M.; Toyota, K.; Fukuda, R.; Hasegawa, J.; Ishida, M.; Nakajima, T.; Honda, Y.; Kitao, O.; Nakai, H.; Klene, M.; Li, X.; Knox, J. E.; Hratchian, H. P.; Cross, J. B.; Adamo, C.; Jaramillo, J.; Gomperts, R.; Stratmann, R. E.; Yazyev, O.; Austin, A. J.; Cammi, R.; Pomelli, C.; Ochterski, J. W.; Ayala, P. Y.; Morokuma, K.; Voth, G. A.; Salvador, P.; Dannenberg, J. J.; Zakrzewski, V. G.; Dapprich, S.; Daniels, A. D.; Strain, M. C.; Farkas, O.; Malick, D. K.; Rabuck, A. D.; Raghavachari, K.; Foresman, J. B.; Ortiz, J. V.; Cui, Q.; Baboul, A. G.; Clifford, S.; Cioslowski, J.; Stefanov, B. B.; Liu, G.; Liashenko, A.; Piskorz, P.; Komaromi, I.; Martin, R. L.; Fox, D. J.; Keith, T.; Al-Laham, M. A.; Peng, C. Y.; Nanayakkara, A.; Challacombe, M.; Gill, P. M. W.; Johnson, B.; Chen, W.; Wong, M. W.; Gonzalez, C.; Pople, J. A. *Gaussian-03*, Revision C.2; Gaussian, Inc.: Pittsburgh, PA, 2003.
(76) Li, X.; Wang, X.; Zhang, L.; Lee, S.; Dai, H. *Science* **2008**, *319*, 1229.
(77) Ferrari, A. C.; Meyer, J. C.; Scardaci, V.; Casiraghi, C.; Lazzeri, M.; Mauri, F.; Piscanec, S.; Jiang, D.; Novoselov, K. S.; Roth, S.; Geim, A. K. *Phys. Rev. Lett.* **2006**, *97*, 187401.
(78) Calizo, I.; Balandin, A. A.; Bao, W.; Miao, F.; Lau, C. N. *Nano Lett.* **2007**, *7*, 2645.

JP808181N